Physicochemical Characteristics of Sago Starch-Chitosan Nanofillers Film

Basirah Fauzi,[a]* Mohd Ghazali Mohd Nawawi,[a] Roslinda Fauzi,[b] and Siti Nur Liyana Mamauod [b]

Starch has potential to be used in new, functional food packaging materials. The attractive factors of starch as a packaging material are its low price and degradable properties. However, brittleness hinders its function as a packaging film. In this study, chitosan nanofillers (CSN) were incorporated into sago starch (SS) formulations to improve the mechanical, physical, and chemical properties of the film. The synthesis of a new formulation from the optimization process resulted in increased mechanical properties; the tensile strength obtained for the sago starch/chitosan nanofillers (SS/CSN) film was 88 MPa compared with 46 MPa for the sago starch film (SSF). In terms of thermogravimetric analysis, the SS/CSN film sustained up to 390 °C with 60% weight loss, whereas SSF experienced a weight loss of 67% at 375 °C. The analyses summarize the concept of using biocomposites to improve the properties of film for the potential purpose in biodegradable packaging plastics.

Keywords: Sago starch; Chitosan Nanofillers; Biocomposite; Film; Biodegradable

Contact information: a: School of Chemical and Energy Engineering, Faculty of Engineering, Universiti Teknologi Malaysia 81310 Skudai, Johor, Malaysia; b: Faculty of Applied Sciences, Universiti Teknologi MARA 40450 Shah Alam, Selangor, Malaysia;
**Corresponding author: basirahfauzi@gmail.com*

INTRODUCTION

The production and practical use of nondegradable plastics contribute to waste disposal problems (Avella *et al.* 2005). Green packaging materials are in high demand to combat these problems and diminish the use of petroleum-based plastics (Oleyaei *et al.* 2016). New inventions of biodegradable packaging materials provide physical protection and create proper physicochemical conditions for food. The major factors to improve biodegradable packaging plastics are to protect food from oxygen, water vapor, ultraviolet light, and both chemical and microbiological contamination (Prasad and Kochhar 2014). New packaging materials are developed to prolong the shelf life of foods and maintain consumer safety by reducing foodborne diseases (Caro *et al.* 2015). After their utilization, it is desirable for the packaging materials to biodegrade in a reasonable period without causing environmental problems.

Starch has received attention as a biodegradable thermoplastic polymer (Lu *et al.* 2006). Products made from agricultural sources such as starch provide alternative ways to develop cheap and attractive degradable materials. In Malaysia, sago starch is obtained exclusively from the sago plant, *Metroxylon sagu*. This type of sago has tremendous potential to be explored in developing biodegradable packaging materials due to its low price in the market (Ahmad *et al*. 1999). The properties of starch-based films and its modification techniques applied to improve the physicochemical and mechanical

properties have been adequately highlighted. As for sago starch, its amylose content is higher than corn and potato starches. This suggests its potential as a good material for food packaging plastics since the properties may provide stronger polymer strength (Nadiha *et al.* 2010). The unique aspect of this work is to use sago starch (SS) as the potential material for producing revolutionary bioplastics filled with polysaccharide nanofillers from chitosan.

Nanotechnology can be defined as the utilization and manipulation of materials with nanometer scale of particle size, which can generate desired properties for novelty applications (Huang *et al*. 2015). Nanocomposites are a new invention for the application to biopolymers in the food packaging industry to reduce the weaknesses of the conventional biodegradable plastics (Abdollahi *et al.* 2013). Biodegradable plastic film is incorporated with nanofillers to improve its properties. Chitosan (CS) is a natural biopolymer that is nontoxic, biodegradable, biocompatible, and a polysaccharide with cationic charges (Onishi and Machida 1999; Kanatt *et al.* 2012). Hence, it is easier to synthesize chitosan into nanoparticles when there is an anionic environment around the polymer (Aider 2010).

This study focuses on the improvement of physicochemical properties as well as generating new systems for sago starch-chitosan nanofillers (SS/CSN) film to prolong its shelf life. These improvements were made with the aim of food preservation of food using biodegradable food packaging. This type of bioplastic is an economical way to address environmental issues associated with traditional packaging.

EXPERIMENTAL

Preparation of SS/CSN Matrix

The SS solution at 2 wt% was formulated by preparing the SS powder in deionized water that contained sorbitol calculated based on the 30 wt% of dry basis of SS. Sorbitol acts as a plasticizer for the purpose of film flexibility. The SS gelatinization was carried out in stirred beakers covered with aluminum foil. The agitation process was performed for 20 min at a constant temperature of 100 °C. The SS paste was cooled to 40 °C to minimize water evaporation. The CSN was synthesized using 0.2 wt% to 0.5 wt% CS reacted with 0.1 wt% of sodium tripolyphosphate (STPP). The solutions were formulated using Design Expert 7.0 software (Stat-Ease, Inc., Minneapolis, MN). After mixing, the mixture was poured onto a casting tray and oven-dried at 60 °C. To control the uniformity of thickness of each sample, the amount of film-forming solutions was maintained at 50 g for each casting plate. The developed films with a constant thickness were stored in 0% relative humidity at 25 °C before the characterization process to maintain the equilibrium of water content inside the films.

Mechanical Properties

The mechanical properties of the developed films were tested according to the ASTM D882-12 (2012) standard with slight modifications. All prepared films were analyzed using a LRX 2.5 KN LLOYD tensile tester (TTS Ltd, Worthington, UK). The film samples were cut into dumbbell shapes with the dimensions of 6.5 cm × 1.0 cm using a hollow die punch. The samples were mounted with a double-sided adhesive tape and clamped between the tensile grips. A constant rate crosshead speed of 10 mm/min was used for the analysis. The values were developed from the average of five replications to ensure the accuracy of the results. The outcome from the tested film was translated into tensile

strength (σ_b), Young's modulus (E), and elongation at break (ε_b).

Thermogravimetric Analysis (TGA)

Thermogravimetric analysis was performed using a thermal analyzer (TGA-400, Perkin Elmer, Waltham, MA). The film samples of approximately 30 mg were heated in an aluminum cell between 50 °C and 500 °C at a heating rate of 10 °C/min in nitrogen atmosphere as the inert gas.

FTIR Analysis

Fourier Transform Infrared (FTIR) spectroscopy (IRTracer-100, Shimadzu, Kyoto, Japan) was used to analyze the absorption frequency of the film. The analysis employed the transmittance-based graph to indicate the functional groups that exist in the film. The reactions of chemical compounds were observed through the peak line produced from the sample. The plastic films were mounted on the steel plate with a resolution of 4 cm^{-1} with attenuated reflectance (ATR) in the spectral range of 4000 cm^{-1} to 600 cm^{-1}. An average of eight scans was taken for each sample to ensure the accuracy of the results.

RESULTS AND DISCUSSION

Mechanical Properties

The analysis of mechanical properties is the most crucial part for the characterization of SS/CSN film. The tensile strength (σ_b), Young's modulus (E), and elongation at break (ε_b) were characterized. Table 1 summarizes the comparison of mechanical properties between the SS/CSN and SSF films.

The synthesis of desired films was conducted on the optimized formulation. The SS/CSN film was formulated from the solution at 100 wt%. The value of tensile strength after the synthesis was 88 MPa, which was similar to the expected value at $p < 0.05$. The comparison between the experimental and predicted results revealed the convincing value for the optimized formulation. Compared with the SSF (46 MPa), the SS/CSN film showed a higher tensile strength. The high tensile strength indicated that the nanofillers were properly dispersed in the matrix (Curvelo *et al*. 2001; Jordan *et al.* 2005).

Table 1. Mechanical Properties of SS/CSN Film and SSF

Properties	SS/CSN Film	SSF
Tensile strength (σ_b) (MPa)	88	46
Young's modulus (E) (MPa)	320	254
Elongation at break (ε_b) (%)	208	132

For the Young's modulus measurements, the optimized formulation of SS/CSN film exhibited the value of 320 MPa, and the control film value was 254 MPa. The presence of nanofillers inside the SS/CSN film and around the compound increased the Young's modulus value. Nanofillers that are dispersed over the matrix may trigger additional stiffness on the developed film and causing the increment of Young's modulus (Pandey *et al*. 2005). Eventually, this value will show the characteristic of a plastic film that aims to be strong and reliable for the application. The elongation at break indicates the stretching ability of plastic films. The SS/CSN film obtained the ε_b value of 208%, while the control

SSF $\mathcal{E}_b$ was 132%. Therefore, the nanofillers provided better reinforcing effects as it has a high surface area to volume ratio (Tang *et al*. 2008), which can create good dispersion in the solution.

Thermogravimetric Analysis

The thermal stability and decomposition temperature of plastic films were evaluated by TGA. Both SSF and SS/CSN films were analyzed at a heating rate of 10 °C/min under nitrogen flow. The temperature used for the analysis was between 50 °C and 500 °C. There were three consecutive stages of film decomposition. The first stage was due to the loss of water, whereas the second stage corresponded to the decomposition of the partially decomposed film. The final stage signified the maximum decomposition phase of the sample. The thermograms for both the SSF and SS/CSN samples showed similar patterns for those three stages. The initial stage for the decomposition was between 50 °C and 150 °C. At this stage, the weight loss for SSF was 4%, whereas the weight loss for the SS/CSN film was 5%. The first stage occurred by the phenomenon of the loosely bound water (Bhat *et al.* 2013).

The second stage of the decomposition occurred at 200 °C. At this stage, the film samples started to decompose by the heat generated. The degradation of the polymer structure caused the depolymerization of amylose in the starch component (Danjaji *et al.* 2001). The weight loss during this stage was 23% for SSF and 31% for the SS/CSN film. Finally, the third stage was examined above 250 °C. The thermograms exhibited the final value of weight loss of 67% at 375 °C for SSF. For the SS/CSN film, the weight loss dramatically increased, but it was achieved at a final temperature of 390 °C for the maximum decomposition. The weight loss for the final stage was 60 % due to the split of the aliphatic ring side chain from the aromatic ring with the breaking of C–C linkages between the CSN structural units (Hosseini *et al.* 2016). The results revealed that the SS/CSN film can sustain at a high temperature environment, hence it is also suitable to be used for heat sealing applications.

Estimation of Functional Groups on Films

The FTIR spectra were used to verify changes in the chemical structure of the SS/CSN film as SS and CSN were incorporated into the formulation. Figure 1 illustrates the different patterns of SSF in comparison with the SS/CSN film. A broad peak of a hydroxyl (O–H) group stretching was observed at 3263 cm^{-1} for the SS/CSN film and 3280 cm^{-1} for SSF. The different peaks between those films demonstrated the increased amount of O–H groups inside the film as the new formulations were developed.

The functional groups of amide I and II appeared at 1642 cm^{-1} and 1565 cm^{-1} corresponding to the conjugated carbonyl (C=O) group stretching and amide (N–H) group bending, respectively. The films differed in terms of the peak spectra shown by SSF at 1641 cm^{-1} for the C=O stretch. The distinct peaks of the films portrayed the incorporation of SS and CSN inside the film. In addition, the SSF spectrum showed a peak for the aromatic ring of C=C at 1413 cm^{-1}. The band was observed to be sharper and shifted to 1414 cm^{-1} after the combination of SS and CSN. The transition of the peak was represented by the presence of CSN, as its chemical structure was in the closed ring of hydrocarbons.

Another characteristic of absorption frequency was shown at 1077 cm^{-1}, which is attributed to C–O stretching in SSF. It became sharper and shifted to 1082 cm^{-1} when other materials were added into the solution. The broad peak at 834 cm^{-1} demonstrated the symmetric P=O of the SS/CSN film. These peaks revealed the crosslinking of CS with

STPP in the transformation of nanoparticles. The CSN was used in the formulation of the film to provide good properties of packaging materials. Therefore, the characterizations of film were absolutely confirmed by the appearance of all functional groups in the FTIR spectra.

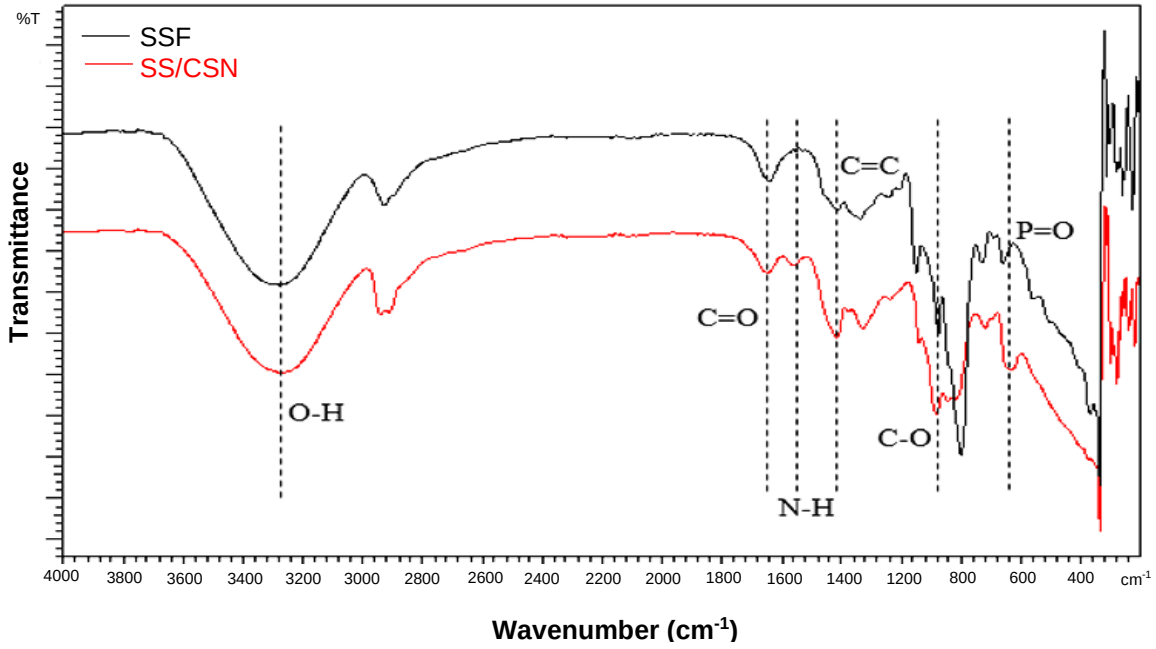

Fig. 1. FTIR Spectra of SSF and SS/CSN Film

CONCLUSIONS

1. Physicochemical characterizations were conducted on the new formulated film developed using the optimized parameters. The mechanical properties of tensile strength, Young's modulus, and elongation at break increased compared to those of the control film. This characteristic is important in order to ensure a plastic film can meticulously be applied for packaging purpose.
2. Thermogravimetric analysis was conducted to analyze the capability of the film to sustain itself in a high temperature environment. The thermograms of both SSF and the formulated SS/CSN film demonstrated the end temperature of the film's degradation of 375 °C and 390 °C, respectively. The weight loss for control film (SSF) was 67%, whereas the SS/CSN film showed 60% of weight loss in the decomposition process. The weight loss and its respective final temperature of film degradation indicated that the developed biocomposite film can be used for heat sealing applications.
3. FTIR spectra described the behavior of food packaging material by showing the chemical structures of the developed film. The functional groups that existed in the FTIR spectra have revealed that there were interactions between the compounds. Therefore, based on the conducted analysis, it is expected that this biodegradable food packaging plastic will provide another viable option to the commercially available food packaging materials.

ACKNOWLEDGEMENTS

The authors fully acknowledge financial support from Ministry of Education under Fundamental Research Grant Scheme, FRGS (R.J130000.7844.4F464) which makes this important research viable and effective.

REFERENCES CITED

Abdollahi, M., Alboofetileh, M., Rezaei, M., and Behrooz, R. (2013). "Comparing physico-mechanical and thermal properties of alginate nanocomposite films reinforced with organic and/or inorganic nanofillers," *Food Hydrocolloids* 32(2), 416-424. DOI: 10.1016/j.foodhyd.2013.02.006

Ahmad, F. B., Williams, P. A., Doublier, J.-L., Durand, S., and Buleon, A. (1999). "Physico-chemical characterisation of sago starch," *Carbohydrate Polymers* 38(4), 361-370. DOI: 10.1016/S0144-8617(98)00123-4

Aider, M. (2010). "Chitosan application for active bio-based films production and potential in the food industry: Review," *LWT - Food Science and Technology* 43(6), 837-842. DOI: 10.1016/j.lwt.2010.01.021

ASTM D882-12 (2012). "Standard test method for tensile properties of thin plastic sheeting," ASTM International, West Conshohocken, United States.

Avella, M., De Vlieger, J. J., Errico, M. E., Fischer, S., Vacca, P., and Volpe, M. G. (2005). "Biodegradable starch/clay nanocomposite films for food packaging applications," *Food Chemistry* 93(3), 467-474. DOI: 10.1016/j.foodchem.2004.10.024

Bhat, R., Abdullah, N., Rozman, H. D., and Tay, G. S. (2013). "Producing novel sago starch based food packaging films by incorporating lignin isolated from oil palm black liquor waste," *Journal of Food Engineering* 119(4), 707-713. DOI: 10.1016/j.jfoodeng.2013.06.043

Caro, N., Quiñonez, E. M., Díaz-Dosque, M., López, L., Abugoch, L., and Tapia, C. (2015). "Novel active packaging based on films of chitosan and chitosan/quinoa protein printed with chitosan-tripolyphosphate-thymol nanoparticles via thermal ink-jet printing," *Food Hydrocolloids* 52, 520-532. DOI: 10.1016/j.foodhyd.2015.07.028

Curvelo, A. A. S., de Carvalho, A. J. F., and Agnelli, J. A. M. (2001). "Thermoplastic starch-cellulosic fibers nanocomposite: Preliminary results," *Carbohydrate Polymers* 45(2), 183-188. DOI: 10.1016/S0144-8617(00)00314-3

Danjaji, I., Nawang, R., Ishiaku, U., Ismail, H., and Ishak, Z. (2001). "Sago starch-filled linear low-density polyethylene (LLDPE) films: Their mechanical properties and water absorption," *Journal of Applied Polymer Science* 79(1), 29-37. DOI: 10.1002/1097-4628(20010103)79:1<29::AID-APP40>3.0.CO;2-R

Hosseini, S. F., Rezaei, M., Zandi, M., and Farahmandghavi, F. (2016). "Development of bioactive fish gelatin/chitosan nanoparticles composite films with antimicrobial properties," *Food Chemistry* 194, 1266-1274. DOI: 10.1016/j.foodchem.2015.09.004

Huang, J.-Y., Li, X., and Zhou, W. (2015). "Safety assessment of nanocomposite for food packaging application," *Trends in Food Science & Technology* 45(2), 187-199. DOI: 10.1016/j.tifs.2015.07.002

Jordan, J., Jacob, K. I., Tannenbaum, R., Sharaf, M. A., and Jasiuk, I. (2005). "Experimental trends in polymer nanocomposites - A review," *Materials Science and*

Engineering: A. 393(1-2), 1-11. DOI: 10.1016/j.msea.2004.09.044

Kanatt, S. R., Rao, M., Chawla, S., and Sharma, A. (2012). "Active chitosan-polyvinyl alcohol films with natural extracts," *Food Hydrocolloids* 29(2), 290-297. DOI: 10.1016/j.foodhyd.2012.03.005

Lu, Y., Weng, L., and Cao, X. (2006). "Morphological, thermal and mechanical properties of ramie crystallites-reinforced plasticized starch biocomposites," *Carbohydrate Polymers* 63(2), 198-204. DOI: 10.1016/j.carbpol.2005.08.027

Nadiha, M. Z. N., Fazilah, A., Bhat, R., and Karim, A. A. (2010). "Comparative susceptibilities of sago , potato and corn starches to alkali treatment," *Food Chemistry* 121(4), 1053-1059. DOI: 10.1016/j.foodchem.2010.01.048.

Oleyaei, S. A., Zahedi, Y., Ghanbarzadeh, B., and Moayedi, A. A. (2016). "Modification of physicochemical and thermal properties of starch films by incorporation of TiO_2 nanoparticles," *International Journal of Biological Macromolecules* 89, 256-264. DOI: 10.1016/j.ijbiomac.2016.04.078

Onishi, H., and Machida, Y. (1999). "Biodegradation and distribution of water-soluble chitosan in mice," *Journal of Biomaterials* 20(2), 175-182. DOI: 10.1016/S0142-9612(98)00159-8

Pandey, J. K., Kumar, A. P., Misra, M., Mohanty, A. K., Drzal, L. T., and Singh, R. P. (2005). "Recent advances in biodegradable nanocomposites," *Journal of Nanoscience and Nanotechnology* 5(4), 497-526. DOI: 10.1166/jnn.2005.111

Prasad, P., and Kochhar, A. (2014). "Active packaging in food industry: A review," *Journal of Environmental Science, Toxicology and Food Technology* 8(5), 1-7. DOI: 10.9790/2402-08530107

Tang, S., Zou, P., Xiong, H., and Tang, H. (2008). "Effect of nano-SiO_2 on the performance of starch/polyvinyl alcohol blend films," *Carbohydrate Polymers* 72(3), 521-526. DOI: 10.1016/j.carbpol.2007.09.019

Article submitted: February 3, 2019; Peer review completed: August 8, 2019; Revised version received: August 20, 2019; Accepted: August 21, 2019; Published: September 3, 2019.
DOI: 10.15376/biores.14.4.8324-8330